Available online at www.sciencedirect.com
ScienceDirect
Journal of Power Sources 180 (2008) 373–379
JOURNAL OF POWER SOURCES
www.elsevier.com/locate/jpowsour

The electrochemical properties of LSM-based cathodes fabricated by electrostatic spray assisted vapour deposition

Jingwang Yan, Xianghui Hou, Kwang-Leong Choy *

School of Mechanical, Materials and Manufacturing Engineering, the University of Nottingham, University Park, Nottingham NG7 2RD, UK

Received 30 November 2007; received in revised form 28 January 2008; accepted 3 February 2008
Available online 10 March 2008

Abstract

$La_{0.8}Sr_{0.2}MnO_{3-\delta}$ (LSM) and LSM–8 mol% yttria-stabilized zirconia (YSZ) composite cathodes were fabricated using electrostatic spray assisted vapour deposition (ESAVD) method. The porous cathode layers of LSM and LSM–YSZ with high specific surface areas were obtained by optimizing the deposition parameters. It was found that the introduction of YSZ into LSM decreased the electrochemical impedance significantly. The activation effect of passing current on the electrochemical activity of the LSM–YSZ composite cathodes was much lower than that of the LSM cathodes. For the LSM–YSZ composite cathodes, there was a saturation of current with increasing applied potential at higher temperatures (from 900 to 1000 °C). The LSM–YSZ composite cathode fabricated by ESAVD exhibited high electrochemical activity at high and intermediate temperatures (from 800 to 1000 °C). This suggests that ESAVD is a promising technique for the fabrication of solid oxide fuel cell (SOFC) cathodes.

Keywords: Solid oxide fuel cell; Cathode; Strontium doped lanthanum manganate; Electrostatic spray assisted vapour deposition

1. Introduction

Lanthanum strontium manganate (LSM) is the most widely used cathode material in solid oxide fuel cells (SOFCs). The oxygen reduction mechanism on LSM and LSM–8 mol% yttria-stabilized zirconia (YSZ) composite cathodes as well as the activity and stability of these types of cathodes have been extensively investigated [1–4]. Several methods have been developed in order to fabricate porous cathodes with high electrochemical performance and good mechanical strength [5–8]. Tape-casting, screen-printing, etc., are commonly applied methods to fabricate cathode layers for SOFCs.

Electrostatic spray assisted vapour deposition (ESAVD) is a variant of the chemical vapour deposition (CVD) process. It involves spraying atomised precursor droplets across an electric field into a heated environment where the charged droplets will undergo decomposition and chemical reaction in the vapour phase. The chemical reactions can be tailored to occur at different zones in order to synthesise dense films, porous coatings or nanocrystalline powders. A wide range of thin and thick coatings with either a dense or porous microstructure for structural and functional applications including indium tin oxide (ITO) [9], TiO_2 films [10–12], $CuInS_2$ films [13], etc., have been deposited using the ESAVD method. Compared with other thin film technologies based on traditional chemical vapour deposition and physical vapour deposition, no vacuum system is required for ESAVD system, thus significantly decreasing the equipment and fabrication costs.

In this paper, ESAVD was used to fabricate LSM and LSM–YSZ composite cathodes for SOFCs. Deposition parameters were optimized to obtain porous cathodes with high specific surface area. The electrochemical performance of the cathodes annealed at various temperatures was characterized by AC impedance spectra and DC polarization. The effect of the introduction of YSZ on the cathode performance was investigated as well.

2. Experimental

$La_{0.8}Sr_{0.2}MnO_{3-\delta}$ (LSM) and LSM–8 mol% yttria-stabilized zirconia (weight ratio 6:4) composite cathodes (5 mm in diameter) were fabricated on 0.5 mm thick YSZ dense substrates (20 mm in diameter) by electrostatic spray assisted vapour deposition method. The precursors for the deposition

* Corresponding author. Tel.: +44 115 9514031; fax: +44 115 9514031.
E-mail address: kwang-leong.choy@nottingham.ac.uk (K.-L. Choy).

0378-7753/$ – see front matter © 2008 Elsevier B.V. All rights reserved.
doi:10.1016/j.jpowsour.2008.02.035

of LSM and YSZ were based on sol solution prepared from metal nitrates. The ratio of LSM and YSZ was controlled by mixing LSM and YSZ precursor in an appropriate volume ratio. The thickness of the cathode layers was controlled by the deposition time. The deposition temperature was controlled at circa 470 °C.

The absorption and desorption properties of the as-deposited cathodes, and cathodes annealed at 900 °C for 2 h were measured by BET method on a surface area and porosity analyzer (Micrometitics ASAP 2020). The phase composition of the as-deposited and annealed cathodes was determined by X-ray diffraction (XRD) using a Siemens D500 X-ray diffractometer. The morphology of the surface and cross-section of the cathodes annealed at various temperatures was characterized using a scanning electron microscope (SEM, Philips XL30). The composition of the films was determined by EDX (Oxford INCAx-Sight 6650 equipped on the SEM system).

A Pt counter electrode with the same size as the cathode and a Pt reference electrode of 0.2 mm^2 were painted on the opposite side of the YSZ disks and sintered at 900 °C for 30 min. The distance between the counter electrode and the reference electrode was controlled at 1.5 mm. AC impedance and polarization behaviours of the cathodes were measured by a Solartron electrochemical system which consisted of an SI 1287 electrochemical interface and a 1255B frequency response analyzer. For AC impedance measurement, a 20 mV AC signal (frequency from 0.01 to 10^6 Hz) was applied to the samples. The experimental data of AC impedance and polarization were collected and analyzed by commercial software Zplot/Zview and Corrware/Corrview, respectively.

3. Results and discussions

The apparatus of the electrostatic spray assisted vapour deposition used to prepare LSM and LSM–YSZ cathodes has been reported elsewhere [14]. The surface morphology of the deposited films can be easily controlled by modifying the key processing parameters. ESAVD is expected to be a promising method for preparing porous cathodes. By adjusting the deposition parameters (for example, the deposition temperature set at circa 470 °C, the precursor concentration set at 0.05 M, the deposition rate set at 10 ml precursor per minute, and the voltage set at 5–12 kV), porous cathodes of LSM and LSM–YSZ were obtained.

Fig. 1 shows the surface morphology and cross-section of an LSM–YSZ cathode fabricated by ESAVD and annealed at 900 °C for 2 h. A similar microstructure was obtained for the LSM cathode deposited under the same conditions. The thickness of the cathodes was circa 40 μm. Cross-section SEM (Fig. 1(b)) shows that LSM–YSZ cathode film adhered well onto YSZ substrate. The cathode layer consisted of clusters of micrometer-scale particles. Such porous structure is desirable for SOFC cathode, which would facilitate the electrochemical reactions at the triple phase boundaries (TPB), and the mass transportation of reactants and products within the cathode layer as well.

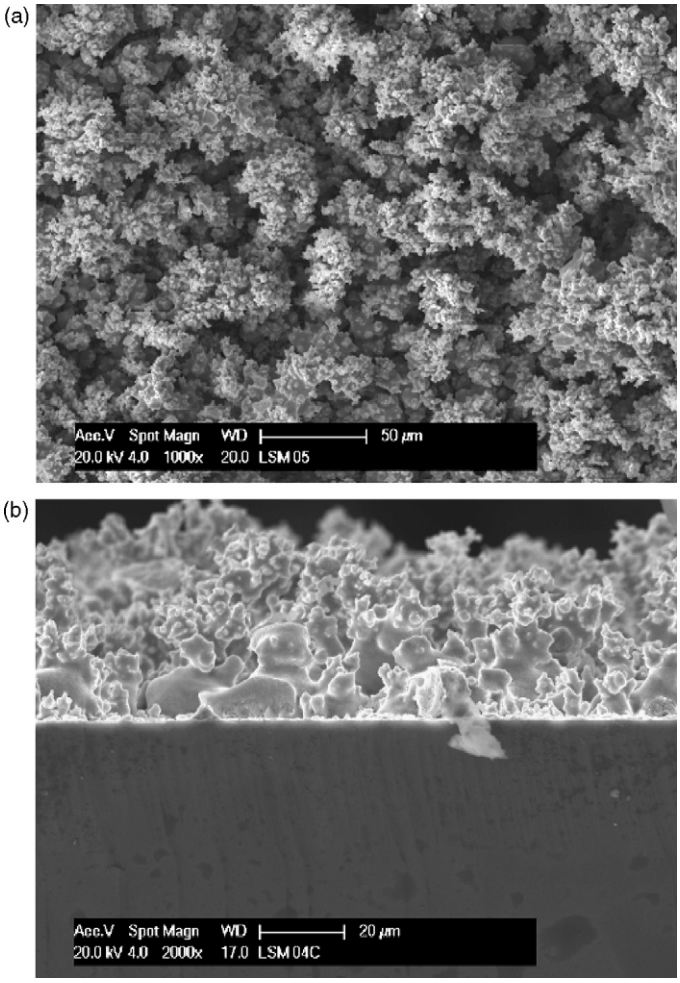

Fig. 1. Surface morphology and cross-section of an LSM–YSZ composite cathode fabricated by ESAVD. The LSM cathode was annealed after deposition at 900 °C for 2 h. (a) Surface; (b) cross-section.

The XRD analysis (Fig. 2) shows that the as-deposited cathodes LSM and LSM–YSZ were amorphous and a perovskite phase of LSM was formed in the LSM cathode after annealing at 900 °C for 2 h. In the LSM–YSZ cathodes annealed under the same condition, only the perovskite phase of LSM and the cubic phase of YSZ were observed, indicating no undesired interfacial reactions between LSM and YSZ substrate can be detected.

BET measurements confirmed that cathodes of LSM and LSM–YSZ have high specific areas as shown in Fig. 3. The specific areas of the annealed LSM and LSM–YSZ cathodes reached 9.37 and 14.66 $m^2\,g^{-1}$, respectively. Although the difference of specific areas of the LSM and LSM–YSZ were not significant, the adsorption and desorption behaviours of these two cathodes were quite different. Different to the pure LSM cathode, the absorption and desorption processes in the LSM–YSZ cathode were more reversible. This indicates that the absorption of the reactants and desorption of the reaction products can easily happen on LSM–YSZ cathodes.

In order to evaluate the performance of the LSM and LSM–YSZ cathodes, AC impedance spectra of these two types of cathodes were measured in oxygen. It is interesting to find out that LSM cathodes showed much lower performance during the

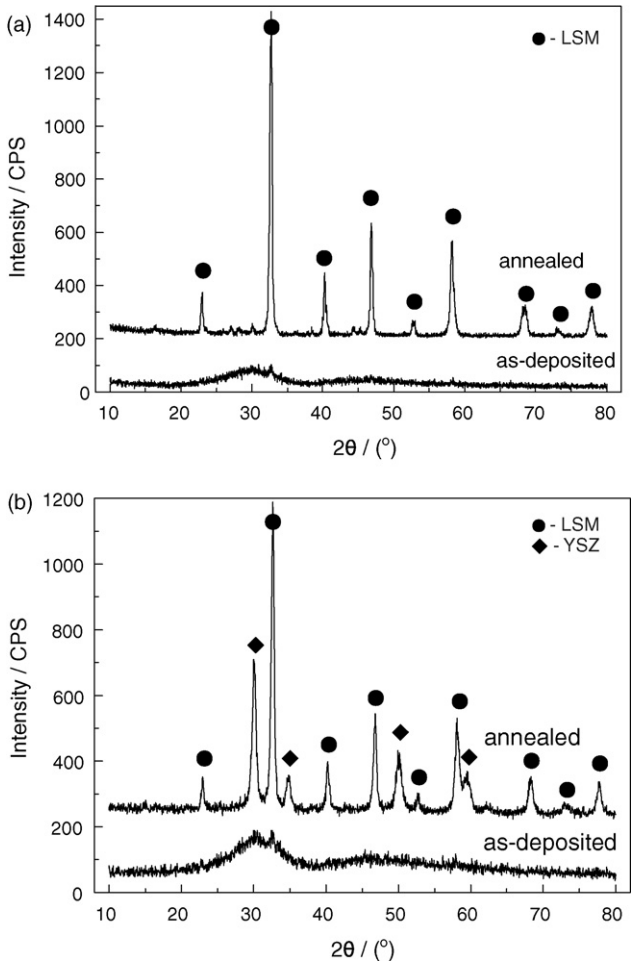

Fig. 2. XRD patterns of the as-deposited and annealed LSM cathodes fabricated by ESAVD. The LSM cathode was annealed 900 °C for 2 h. (a) LSM cathode; (b) LSM–YSZ cathode.

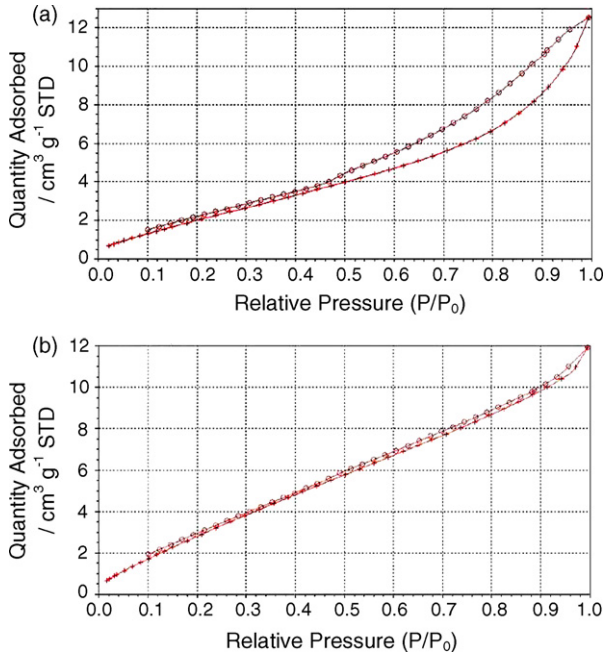

Fig. 3. Absorption and desorption properties of the LSM and LSM–YSZ composite cathodes measured by BET method. (a) LSM cathode; (b) LSM–YSZ cathode.

first measurement but the performance increased rapidly after a current was passed through the cathode. From the AC impedance spectra shown in Fig. 4, we notice that the electrochemical resistance was increased by about one order. However, the change of the contact ohmic resistance was nearly negligible. The passing current increased the electrochemical activity of the cathode, but did not change the IR drop and the contact resistance between the cathode layer and the electrolyte substrate. The promotion effect of the passing current is considered to be possibly induced by the change of the grain boundary in the LSM layer and the TPB length between the LSM, YSZ and the gaseous phase.

Fig. 5 shows the AC impedance spectra of the LSM cathode at various temperatures. With increasing temperature, both the ohmic resistance and electrochemical resistance of the LSM cathode decreased. At high frequency, obvious arcs (consisting of several semi-circles) were formed and the arcs were compressed to a line at low frequency. This means that the contribution from the capacitor between the cathode and the electrolyte layers nearly disappeared and only the resistance related with the absorption, desorption and electrochemical processes changed slightly with the frequency. As a result of the high specific area of the cathode, no concentration polarization was observed. This result also indicates a good contact between the electrode and electrolyte.

The spectra of the LSM cathode at lower temperatures obviously consisted of two semi-circles. With increasing temperature, the semi-circle at medium frequency decreased and finally disappeared at temperatures above 800 °C. It suggests that at high temperatures (i.e. above 800 °C), the electrochemical reaction is the dominant step to the whole electrode process,

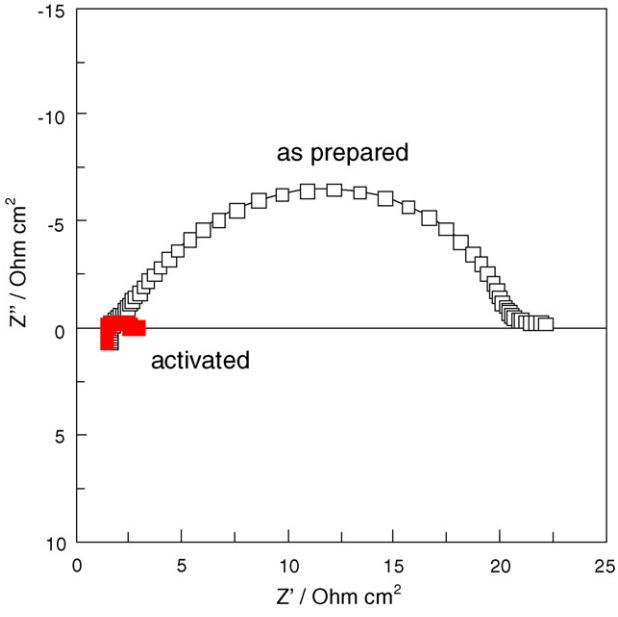

Fig. 4. AC impedance spectra of the as-prepared and activated LSM cathodes at 800 °C.

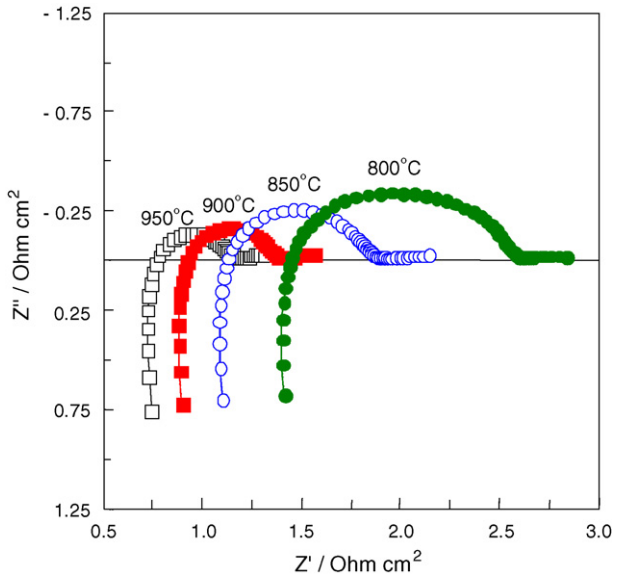

Fig. 5. AC impedance spectra of the activated LSM cathode at different temperatures.

and with the decrease of temperature, the effect from the surface absorption process is increased.

Fig. 6 shows the polarization behaviour of the LSM electrodes at different temperatures. During SOFC operation, the potential of the cathode is always reduced by the passing current, so only the polarization curves under negative current are plotted in this figure. The current density increased rapidly with the increase of the polarizing potential when this potential was lower than 0.155 mV. Further increasing the polarizing potential, the current density increased gradually. The higher polarizing voltage also led to a higher responding current.

Fig. 7 shows the AC impedance spectra of the as-prepared and activated LSM–YSZ cathodes at 1000 and 800 °C, respectively. For LSM–YSZ composite cathodes, the activation effect on the electrode activity was not significant, which was rather different to that of the pure LSM cathodes. This result suggested that there were sufficient electrochemically active sites in the as-prepared

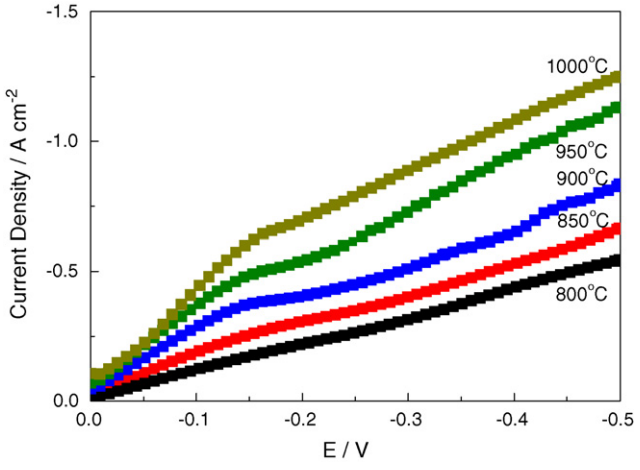

Fig. 6. Polarization curves of the activated LSM cathode at different temperatures.

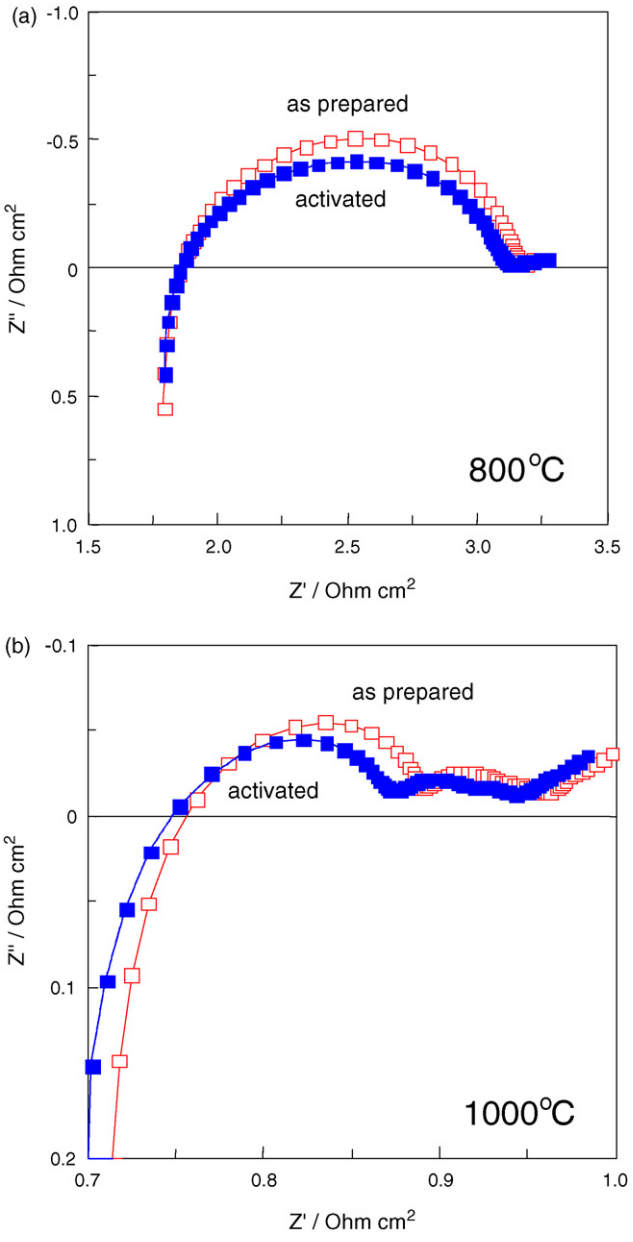

Fig. 7. AC impedance spectra of the as-prepared and activated LSM–YSZ cathodes at (a) 800 and (b) 1000 °C, respectively.

LSM–YSZ composite electrodes. No improvement on the electrode performance after passing a constant current indicated the electrode microstructure was more stable than that of LSM cathodes. Two semi-circles can be observed on the spectra of the LSM–YSZ cathode at much higher temperature (e.g. 1000 °C), indicating the adsorption and desorption processes were still important factors to the total electrode performance even though the electrochemical activity was much improved at high temperature. The concentration polarization also appeared on the spectra of the LSM–YSZ cathode at 1000 °C. The total resistance of the cathode was only 0.2 Ω cm^2 at 1000 °C, which was much lower than that of the cathode at 800 °C (circa 1.3 Ω cm^2). However, at 800 °C only one semi-circle can be observed, which means at lower temperatures the electrochemical process dominated the whole electrode performance and the contribution

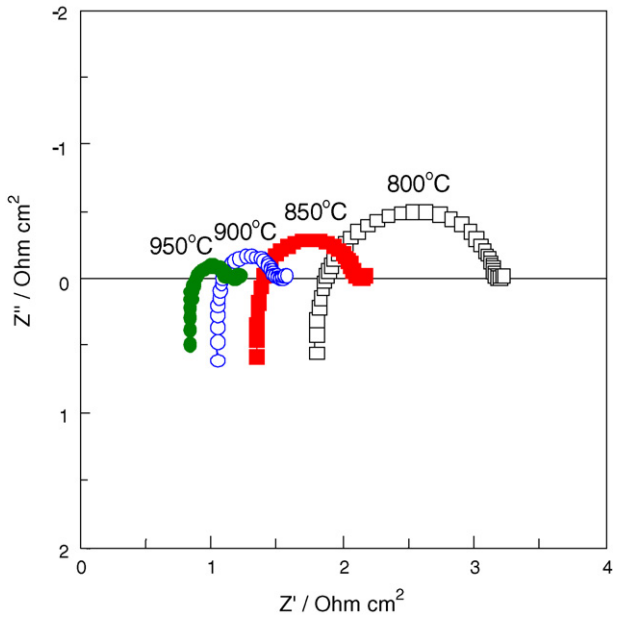

Fig. 8. AC impedance spectra of the activated LSM–YSZ composite cathode at different temperatures.

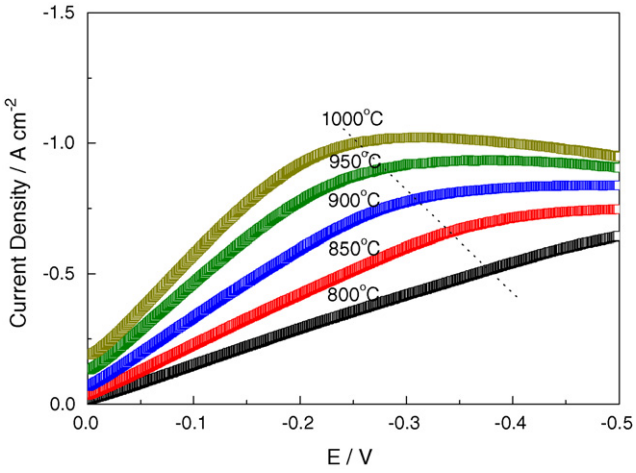

Fig. 9. Polarization curves of the activated LSM–YSZ composite cathode at different temperatures.

from the mass transportation, absorption and desorption on the electrode can be ignored. In addition, intermediate temperature SOFCs (IT-SOFCs) are normally operated at a temperature lower than 800 °C, so the microstructure of the LSM–YSZ composite cathodes with high porosity and specific surface area fabricated by ESAVD is suitable for IT-SOFCs.

The AC impedance spectra at various temperatures of the LSM–YSZ composite cathodes (weight ratio between LSM and YSZ = 6/4) fabricated by ESAVD are shown in Fig. 8. The spectra of cathodes at various temperatures look similar, despite both the electrode resistance and the IR drop in the half cells increased with decreasing temperature. The electrode resistance was ca. 0.4 Ω cm^2 at 950 °C and sharply increased to 1.3 Ω cm^2 when the temperature dropped to 800 °C. It is expected the output performance of a SOFC using an LSM–YSZ composite cathode is lower at intermediate temperatures than that at higher temperatures. The total electrode resistance at immediate temperature is not high. Therefore, a good output performance for an IT-SOFC using a LSM–YSZ composite cathode produced by ESAVD could be obtained if a thin layer electrolyte film is being fabricated.

The polarizing behaviour of the LSM–YSZ composite cathodes at different temperatures is shown in Fig. 9. At 800 °C the current density changed linearly with the supplied potential between the cathode and the reference electrode. The current density under a specific potential bias increased with increasing temperature. A saturation current density was observed above 850 °C and with increasing temperature, the saturation current density was reached at a lower applied potential bias. At higher temperature the current density reached a maximum value quickly with the increase of the applied potential. In addition, further increasing the potential can only introduce a very small increase of current density at 850 °C and will keep the current density constant at 900 °C after the turning point was reached. It should be noted that at 900 and 950 °C the current density decreased with increasing the applied potential after the maximum current density was reached. The decrease at 950 °C is lower than that at 1000 °C. This result suggests that at each temperature there is a saturation current density and at a higher temperature the saturation current density can be reached at a lower potential bias. This decrease of the current density at high temperature is introduced by the decrease of the electrode activity and the increase of the electrode resistance. XRD measurements confirmed that this was related to the formation of the reaction product $La_2Zr_4O_7$ which occurred in the LSM–YSZ composite electrodes at high temperatures, along with the microstructure change of the cathode layer at high potential bias (high electrical current passes the electrode which causes a much higher electrode temperature, i.e. the actual cathode temperature is higher than that of the measured value). As a comparison, the decrease of current density was observed with the increase of the applied potential because $La_2Zr_4O_7$ formation reaction occurred in the LSM–YSZ electrodes.

In order to further clarify the promotion effect on the electrochemical performance of SOFC cathodes by introducing YSZ into LSM, the comparison of the AC impedance spectra between the LSM and LSM–YSZ cathodes at relatively low temperatures (600 and 700 °C) was carried out. As shown in Fig. 10, at higher temperatures, it is difficult to investigate some rapid processes. According to the present understanding of LSM-based electrodes, an equivalent circuit is proposed for the LSM and LSM–YSZ electrodes and shown in Fig. 11. In order to simulate the electrode processes, constant phase elements (CPE) were introduced into the equivalent circuit. CPE is a simple distributed element which produces impedance having a constant phase angle in the complex plane. T and P are two parameters in the mathematic expression of the impedance of CPE components shown below,

$$Z(\mathrm{CPE}) = \frac{1}{T(\omega i)^P}.$$

The exponent P determines this angle. In the special case of $P = 1$, the CPE acts like a capacitor with T equal to the capaci-

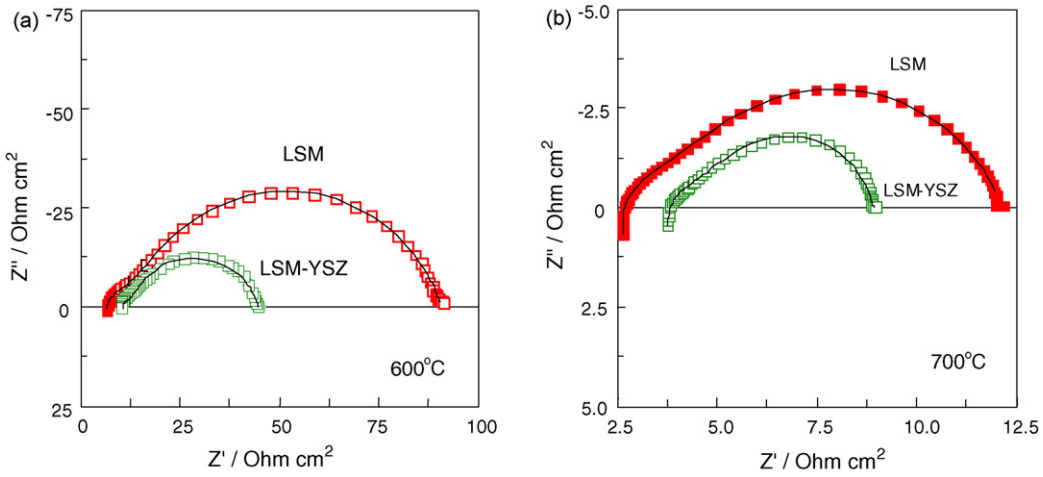

Fig. 10. Comparison of the AC impedance spectra of the activated LSM and LSM–YSZ cathodes at (a) 600 and (b) 700 °C. Open and solid squares are the experimental data and the lines are for the fitting results.

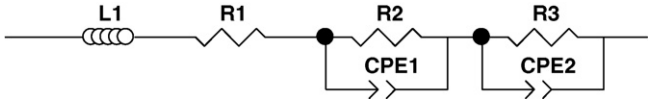

Fig. 11. Equivalent circuit for the activated LSM and LSM–YSZ cathodes.

tance. The CPE can also yield an inductance when $P = -1$, or a resistance when $P = 0$.

The fitting results for the AC impedance spectra of the cathodes to this equivalent circuit at 600 and 700 °C are shown in Table 1, which are also illuminated as lines in Fig. 10. In Table 1, CPE1-T and CPE2-T represent T for CPE1 and CPE2, and CPE1-P and CPE2-P represent P for CPE1 and CPE2, respectively. The inductance $L1$ for these two electrodes at all the temperatures was very close, which was introduced by the electrochemical measurement system. The high frequency semicircle was related to the electrochemical processes occurring in the electrodes. For LSM cathode, when the temperature was reduced from 700 to 600 °C, $R2$ changed from 1.55 to 7.25, and the difference was about 4.7 times. However, for LSM–YSZ composite cathode, the change of $R2$ was much smaller, which was only 1.12 times, when the temperature decreased from 700 to 600 °C. Compared with the pure LSM cathode, the electrochemical activity of the LSM–YSZ composite cathode was not so temperature-dependant. The changes of $R3$, which is considered as the absorption/desorption resistance on the electrodes, were very close for the LSM and LSM–YSZ composite cathodes (ca. 10 times) when the temperature decreased from 700 to 600 °C, despite the absolute value for the LSM–YSZ cathode was nearly one half that for LSM pure cathode. This indicates that the introduction of the YSZ facilitated the absorption and desorption processes on the electrodes. It means the expansion of the triple phase boundary (TPB) by adding YSZ can shorten the migrating distance of the absorbed species before and after reaction occurred at TPB.

Table 1
Fitting results for the LSM and LSM–YSZ cathodes at 600 and 700 °C

	LSM		LSM–YSZ	
	600 °C	700 °C	600 °C	700 °C
$L1$ (H)	1.39×10^{-6}	1.42×10^{-6}	1.10×10^{-6}	1.11×10^{-6}
$R1$ (Ω)	6.58	2.61	10.58	3.65
$R2$ (Ω)	7.25	1.55	2.09	1.86
CPE1-T	9.2×10^{-4}	1.8×10^{-3}	2.6×10^{-4}	2.7×10^{-3}
CPE1-P	0.79	0.73	0.80	0.59
$R3$ (Ω)	76.83	7.98	32.03	3.15
CPE2-T	1.9×10^{-3}	2.8×10^{-3}	4.5×10^{-4}	6.7×10^{-4}
CPE2-P	0.82	0.79	0.83	0.93

It is obvious that the effects of the YSZ and temperature on the constant phase elements (i.e. CPE-1 and CPE-2) are not so obvious compared with that on ohmic resistances, $R2$ and $R3$. Hence, the improvement of the cathode performance by introducing YSZ was mainly caused by the reduction of absorption/desorption resistance in the electrodes. This effect turned out to be much more significant at lower temperatures.

4. Conclusions

Electrostatic spray assisted vapour deposition is a promising method to fabricate LSM-based cathodes for solid oxide fuel cells (SOFCs). LSM and LSM–YSZ cathodes with high porosity and specific surface area have been successfully deposited by ESAVD. The as-deposited films were amorphous and become crystalline after annealing in air at 900 °C for 30 min. For the LSM cathodes fabricated by ESAVD, passing current promotes the electrode performance significantly. For the LSM–YSZ cathodes fabricated by ESAVD, the promotion of the passing current on the electrode performance is negligible. The YSZ in the cathode slightly increases the IR drop but clearly decreases the electrochemical resistance.

Acknowledgement

The authors would like to acknowledge the financial support provided by EPSRC on Supergen Fuel Cells-Powering a Greener Future (EP/C002601/1).

References

[1] S.J. Skinner, Int. J. Inorg. Mater. 3 (2001) 113–121.
[2] J.V. Herle, A.J. McEvoy, K.R. Thampi, Electrochim. Acta 41 (1996) 1447–1454.
[3] Y. Jiang, S.Z. Wang, Y.H. Zhang, J.W. Yan, W.Z. Li, Solid State Ionics 110 (1998) 111–119.
[4] S.P. Jiang, J. Power Sources 124 (2003) 390–402.
[5] C.J. Li, C.X. Li, M. Wang, Surf. Coat. Technol. 198 (2005) 278–282.
[6] S.W. Zha, Y.L. Zhang, M.L. Liu, Solid State Ionics 176 (2005) 25–31.
[7] S. Charojrochkul, K.L. Choy, B.C.H. Steele, J. Eur. Ceram. Soc. 24 (2004) 2515–2526.
[8] N. Caillol, M. Pijolat, E. Siebert, Appl. Surf. Sci. 253 (2007) 4641–4648.
[9] R. Chandrasekhar, K.L. Choy, Thin Solid Films 398/399 (2001) 59–64.
[10] J. Du, K.L. Choy, Solid State Ionics 173 (2004) 119–124.
[11] X.H. Hou, K.L. Choy, Surf. Coat. Technol. 180/181 (2004) 15–19.
[12] X.H. Hou, K.L. Choy, Mater. Sci. Eng. C 25 (2005) 669–674.
[13] X.H. Hou, K.L. Choy, Thin Solid Films 480 (2005) 13–18.
[14] K.L. Choy, Prog. Mater. Sci. 48 (2003) 57–170.